
This copy is for your personal, non-commercial use only.

If you wish to distribute this article to others, you can order high-quality copies for your colleagues, clients, or customers by [clicking here](#).

Permission to republish or repurpose articles or portions of articles can be obtained by following the guidelines [here](#).

The following resources related to this article are available online at www.sciencemag.org (this information is current as of August 22, 2014):

Updated information and services, including high-resolution figures, can be found in the online version of this article at:

<http://www.sciencemag.org/content/301/5636/1087.full.html>

This article **cites 27 articles**, 4 of which can be accessed free:

<http://www.sciencemag.org/content/301/5636/1087.full.html#ref-list-1>

This article has been **cited by** 73 article(s) on the ISI Web of Science

This article has been **cited by** 8 articles hosted by HighWire Press; see:

<http://www.sciencemag.org/content/301/5636/1087.full.html#related-urls>

This article appears in the following **subject collections**:

Geochemistry, Geophysics

http://www.sciencemag.org/cgi/collection/geochem_phys

22. B. M. Jakosky *et al.*, *Geophys. Res. Lett.* **17**, 985 (1990).
23. Several investigations have tentatively identified carbonate absorptions in the atmospheric dust based on telescopic data sets (31, 32). The number of spectra collected is limited and the large footprints include a wide range of surface temperatures, making the data difficult to interpret. These absorptions are inconsistent with Mariner 6/7 IRS, Mariner 9 IRIS, and MGS TES data, which all produce consistent spectral features and are considered well calibrated.
24. J. L. Bandfield, *J. Geophys. Res.*, 2001JE001510 (2002).
25. J. L. Bandfield, V. E. Hamilton, P. R. Christensen, *Science* **287**, 1626 (2000).
26. R. Kahn, *Icarus* **62**, 175 (1985).
27. F. P. Fanale *et al.*, in *Mars*, H. H. Kieffer, B. M. Jakosky, C. W. Snyder, M. S. Matthews, Eds. (Univ. of Arizona Press, Tucson, 1992), pp. 1135–1179.
28. O. B. Toon, J. B. Pollack, W. Ward, K. Bilski, *Icarus*, **44**, 552 (1980).
29. F. P. Fanale, J. R. Salvail, W. B. Banerdt, R. S. Saunders, *Icarus* **50**, 381 (1982).
30. J. B. Pollack, J. F. Kasting, S. M. Richardson, K. Poliakoff, *Icarus* **71**, 203 (1987).
31. E. Lellouch *et al.*, *Planet. Space Sci.* **48**, 1393 (2000).
32. J. B. Pollack *et al.*, *J. Geophys. Res.* **95**, 14595 (1990).
33. We thank M. Kraft, M. Smith, J. Pearl, P. Niles, L. Leshin, V. Hamilton, A. Baldridge, and S. Ruff for

discussions that significantly improved the manuscript. K. Bender, K. Homan, K. Murray, N. Gorelick, S. Anwar, and H. Moncrief provided operations and software support necessary for the TES investigation. R. Clark and an anonymous reviewer provided helpful discussion and comments that improved the clarity of the data presented here.

Supporting Online Material

www.sciencemag.org/cgi/content/full/301/5636/1084/DC1

Materials and Methods

SOM Text

Figs. S1 and S2

16 June 2003; accepted 18 July 2003

Tidally Controlled Stick-Slip Discharge of a West Antarctic Ice Stream

Robert A. Bindschadler,^{1*} Matt A. King,² Richard B. Alley,³ Sridhar Anandakrishnan,³ Laurence Padman⁴

A major West Antarctic ice stream discharges by sudden and brief periods of very rapid motion paced by oceanic tidal oscillations of about 1 meter. Acceleration to speeds greater than 1 meter per hour and deceleration back to a stationary state occur in minutes or less. Slip propagates at approximately 88 meters per second, suggestive of a shear wave traveling within the subglacial till. A model of an episodically slipping friction-locked fault reproduces the observed quasi-periodic event timing, demonstrating an ice stream's ability to change speed rapidly and its extreme sensitivity to subglacial conditions and variations in sea level.

Concern that the West Antarctic Ice Sheet did, does, and will contribute to increasing sea level has driven two decades of extensive research on ice-flow dynamics (1, 2). Evidence for periods of rapid retreat abounds (3–5). Currently northward-draining parts of this ice sheet are thinning rapidly, but not at rates sufficient to provide a large fraction of the present rate of sea level rise (6). The rest of the ice sheet is now close to equilibrium or slightly thickening (7, 8).

For the West Antarctic Ice Sheet to raise sea level rapidly in the near future would require a substantial acceleration of its ice streams, the fast-moving rivers of ice that discharge much of the ice sheet back into the oceans (9). Some of these outlets are accelerating or have accelerated recently (10). Elsewhere, the major ice streams

feeding the Ross Ice Shelf have either stopped, are decelerating, or are maintaining their velocity (7). In the case of Whillans Ice Stream (WIS), the current rate of deceleration is 1 to 2% per year, a rate that would result in stagnation if sustained over the next 50 to 100 years.

Recent field global positioning system (GPS) measurements from a 2-week survey on the “ice plain” in the mouth of WIS revealed that this portion of the ice stream moves by brief, rapid motion events separated by extended periods of no motion (11). Position solutions every 5 min illustrate this stick-slip motion of the ice plain (Fig. 1) (12). Quiescent periods were from 6 to 18 hours long. Slip events lasted from 10 to 30 min, during which the ice moved downstream a distance of a few tens of centimeters at rates of about 1 meter per hour, at least 30 times faster than the already high velocity of the ice stream feeding the ice plain. There was no measurable vertical motion associated with this phenomenon. For any particular site, flow reached approximately the same speed during each slip event. These speeds corresponded closely to the speeds calculated assuming a frictionless bed (13). Differential processing of GPS data for pairs of

stations permitted a finer temporal view of the evolution of slip events (14). Acceleration to frictionless speeds was accomplished in as little as 30 s, the limiting temporal resolution. Deceleration was somewhat slower, but usually occurred within 2 to 5 min. Minor upstream rebound also was observed in the first hour of stagnation, typically amounting to about 10% of the downstream displacement.

Slip occurred across the ice plain, but was not exactly synchronous. Interpolation of slip displacements from the 5-min positions at up to five simultaneously occupied stations produced typical lags of a few minutes between the times of maximum speed. To quantify the speed and direction of this propagation effect, trios of sites were examined (15). From 17 sets of data, a mean speed of propagation of 88 ± 79 m/s was determined. This speed is close to the 150 m/s shear wave speed measured in the subglacial till farther upstream (16). The large uncertainty may represent some spatial heterogeneity in the propagation effect. The general direction of plane wave propagation was northward, nearly transverse across the ice plain, but there were significant variations from this direction. The propagation through the floating ice shelf is probably as a much faster-moving elastic body wave because the ice shelf coupling to water is inefficient (17).

A few deviations from stick-slip behavior were noticed, all at the edges of the ice plain (18). During periods of no motion on the ice plain, ice-shelf stations moved gradually downstream with larger displacements in synchrony with slips of the grounded ice plain. Occupation times at most sites were short, spanning only two to four slip events; therefore, a full characterization must await subsequent field studies.

There is a clear association between this stick-slip phenomenon and the ocean tide, which has a dominant diurnal component beneath the Ross Ice Shelf (19). During the survey, the tidal cycle ranged from weak, neap tides with a minimum amplitude of 0.15 m to a nearly 1-m amplitude during

¹Ocean and Ice Branch, NASA Goddard Space Flight Center, Greenbelt, MD 20771, USA. ²School of Civil Engineering and Geosciences, University of Newcastle, Newcastle Upon Tyne, NE1 7RU, UK. ³Department of Geosciences and EMS Environment Institute, Pennsylvania State University, University Park, PA 16802, USA. ⁴Earth and Space Research, Seattle, WA 98102–3620, USA.

*To whom correspondence should be addressed. E-mail: Robert.A.Bindschadler@nasa.gov

REPORTS

the following spring tide. A continuous record of the tide was not available, so a model was used (20). Our GPS data from ice-shelf sites confirmed the tidal phase, but measured magnitudes were smaller than calculated, probably due to proximity to grounded ice.

During spring tides, the occurrence of slip events for most grounded ice plain sites was extremely regular, with one event shortly after high tide followed by a second event in the middle or toward the end of falling tide (Fig. 2). Roughly half of the average daily motion occurred during each event. During neap tides, this periodicity broke down, including some otherwise unobserved events on the rising tide (Fig. 2). Tidal influence on ice flow has been observed on tidewater glaciers, with the faster speeds occurring during the lower portion of the tidal cycle (21–23). Tidally synchronous flow variations have also been seen on

floating ice shelves (24). Nearby ice streams C and D also show flow response in antiphase to tidal variation. On ice stream D, GPS data show a $\pm 50\%$ variation in flow speed (25). Ice stream C still moves primarily by basal processes, rather than by internal deformation, but slowed about 150 years ago to a speed for which collected GPS data are not sufficiently accurate to reliably capture the tidal variations in flow; however, basal seismicity caused by motion of the ice stream is modulated by the tide and peaks near the grounding line at low tide (26). In contrast to data from the WIS ice plain, C and D show upglacier propagation and damping of the tidal signal, with much lower propagation velocities of 1.5 m/s on C and 5.6 m/s on D.

A consistent interpretation of these observations is that till beneath C and D is behaving as a (pseudo)viscous material whereas that under WIS is behaving in a

plastic or frictional manner (27). The slow propagation velocities on C and D are consistent with viscous delay by subglacial till of an elastic wave in ice (although additional modeling is planned for D to better quantify the role of the ice-stream sides as well as the basal till in slowing the propagation). Nonsteady conditions in a dilatant Coulomb-plastic till can introduce a strain-rate dependence on stress, or pseudo-viscosity (28–30). Increased deformation at a point in till can produce dilatancy, water-pressure drop, and strengthening of that till until water inflow is complete. The greater the stress, the greater the strengthening of the till, up to some failure level. Exceedance of the failure level (which is lowered by approach to steady state) allows the usual plastic behavior of the till to be evident.

Regions of enhanced basal resistance to flow, or “sticky spots,” can be caused by bedrock asperities sticking through till or perhaps by other processes (31). Repeated microearthquakes from specific sites beneath C show that such sticky spots are common (32), so breakage of one or a few may not raise the stress on intervening till to the failure level. Partial restraint of ice stream D by its sides may also keep basal stress on till there below the failure level. However, the thick till (33) of the ice plain of WIS likely has left the region with very few sticky spots, and the great width limits the effect of side drag; therefore, breakage of one or a few sticky spots could load the till past failure and thus expose the plastic nature.

To test this hypothesis for the WIS ice plain, we constructed a simple model that balances the forces encouraging and resisting the motion of an ice plain resting on a plastic till. The motion of the ice stream (speed V) presses on the ice plain (thickness H and length L) at a constant rate as

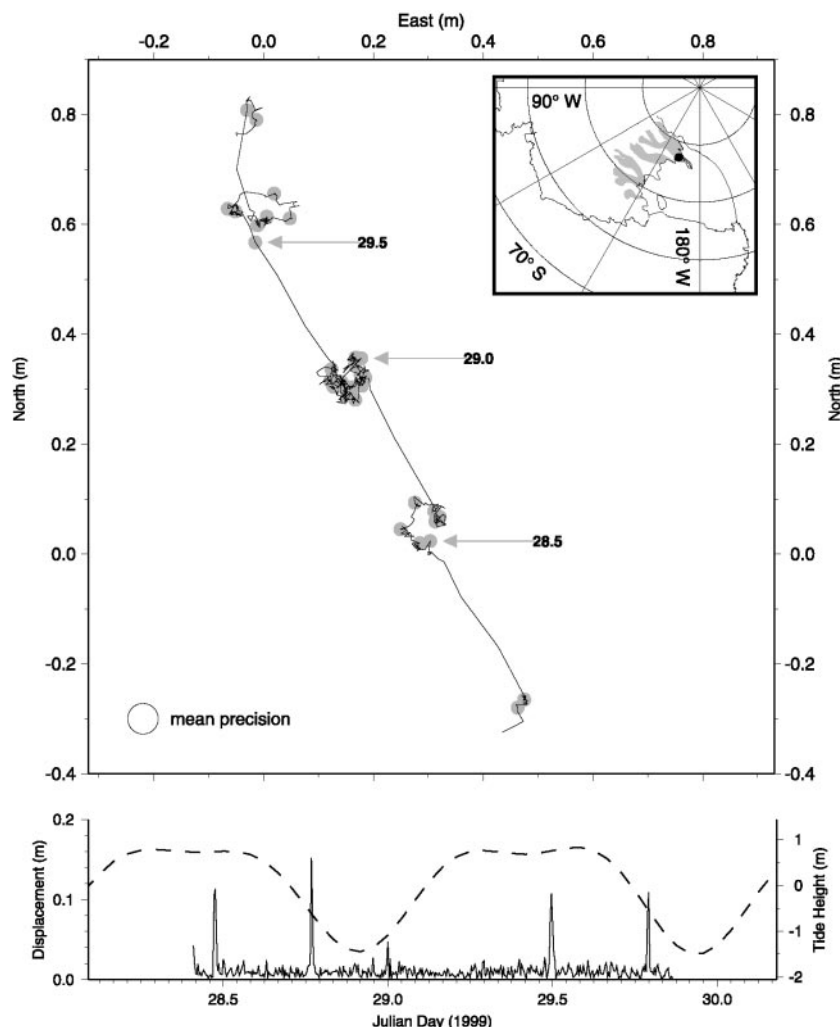


Fig. 1. Motion of site G2. (Top) Horizontal position every 5 min connected by straight lines. Gray dots indicate the beginning of each hour with Julian day indicated by arrows. Inset shows location of ice streams (shaded) and site G2 (solid circle). (Bottom) Horizontal displacement (solid line) between successive 5-min positions and modeled ocean tide (dashed line) at a nearby location.

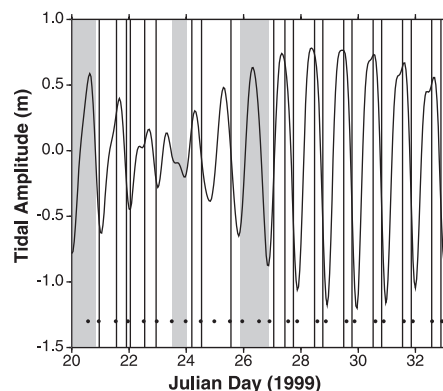


Fig. 2. Comparison of observed slip events (vertical lines) and predicted slip events (solid circles) superimposed on tidal height at station J10. Shaded areas are times when no observations were made.

ice tries to move downstream. The stored elastic strain (Vt/L) is transferred to shear along the base of the ice plain according to the elastic modulus of ice (E) and the ratio of ice thickness to ice-plain length (H/L). The rising and falling ocean tide (h) change the height of the water column the ice plain must displace to move, affecting the resistance to downstream motion. This resistance can also be viewed as a shear stress distributed over the base of the ice plain. The fundamental model equation is

$$\tau_b = \tau_0 + E \left(\frac{HV}{L^2} \right) (t - t_0) - \rho g \left(\frac{H}{L} \right) h(t)$$

where τ_b is the shear stress at the base of ice; τ_0 is an initial, minimum shear stress; ρ is ice density; g is gravitational acceleration; and t is time, with t_0 as the initial time. Stress increases with time, modulated by the tidal resistance, until the yield stress of 4 kPa is reached and a slip event occurs (34). Slip relieves some of the stress, decreasing it to τ_0 , a value below the combined strength of till and sticky spots, which stops the slip.

Our observation that, during spring tides, two slip events occur during a diurnal tidal cycle was used to calculate a stress drop of 0.3 kPa per slip event (35). If there were no tides at all, slip events would be predicted to occur approximately every 12 hours. However, the varying tidal amplitude disrupts this simple regularity.

Input of the modeled tide during the 2-week observation period produces a series of predicted slip events that closely matches the observations (Fig. 2) (36). During spring tides, the larger tidal amplitude delays the slip event as the tide rises but eventually allows release once the rate of rise has declined and the stored elastic strain has exceeded this resistance. On the rapidly falling tide, resistance to slip is diminished so quickly that a second slip event occurs before low tide is reached. During neap tides, variability of tidal resistance is smaller so elastic strain increases more rapidly than resistance even on the rising tide, making slip events on the rising tide possible.

The agreement of our model with observations is robust. Changes of 10% in parameter values have little bearing on the results. Factor-of-two changes in the input parameters radically alter the resulting predictions to the point that all similarity with observations is lost.

Our observations of stick-slip motion support the existence of a plastic character of the underlying till. Our model supports the simple concepts that the tidal oscillations provide the resistance that controls the timing of slip events and that slip events are associated with the release of stored

elastic strain that decreases the subglacial shear stress, followed by a period in which additional elastic strain is stored before the next slip event can take place. Our plastic rheology model of WIS ice plain and the viscous rheology models of C and D both are potentially consistent with a model of Coulomb-plastic till with strain-rate dependence on stress from dilatancy at low stresses under nonsteady conditions.

The connection between relatively minor tidal fluctuations and enormous speed variations emphasizes the delicate balance of forces and extreme sensitivity at play in the mouth of an ice stream. Tidal oscillations provide a sensitive probe of critical basal processes that will be exploited in recently approved new field work to further characterize these events and their implications. Of special interest are the relations between this behavior and the long-term evolution of the ice streams. Ice stream D appears to be maintaining speed, WIS is slowing, and ice stream C has nearly stopped. These long-term changes undoubtedly involve the same ice-till-water system that dictates the stick-slip behavior reported here. Links will be sought between the processes that force ice-stream behavior on diurnal, decadal, and millennial time scales.

References and Notes

1. R. A. Alley, R. A. Bindschadler, *Antarct. Res. Ser.* **77**, 1 (2001).
2. R. A. Bindschadler, C. R. Bentley, *Sci. Am.* **287**, 98 (2002).
3. H. Conway, B. L. Hall, G. H. Denton, *Science* **286**, 180, (1999).
4. T. B. Kellogg, D. E. Kellogg, *J. Geophys. Res.* **92**, 8859 (1987).
5. J. B. Anderson, S. S. Shipp, L. Bartek, D. E. Reid, *Antarct. Res. Ser.* **57**, 39, (1992).
6. A. Shepherd, D. J. Wingham, J. A. D. Mansley, *Geophys. Res. Lett.* **29**, 1364 (2002).
7. I. Joughin, S. Tulaczyk, *Science* **295**, 476 (2002).
8. E. Rignot, R. H. Thomas, *Science* **297**, 1502 (2002).
9. C. R. Bentley, *Science* **275**, 1077 (1997).
10. E. Rignot, M. Schmeltz, *Ann. Glaciol.* **34**, 189, (2002).
11. R. A. Bindschadler, P. L. Vornberger, M. A. King, L. Padman, *Ann. Glaciol.* **36**, 263 (2003). The mouth of WIS is a promontory of a lightly grounded "ice plain" approximately 100 km long and 50 km wide, surrounded by the floating Ross Ice Shelf and ending in the well-grounded Cray Ice Rise. The 29-site survey was conducted from 21 January 1999 to 2 February 1999 using five Ashtech Z-12 receivers simultaneously occupying various sites on the ice plain and the nearby ice shelf. Occupation time varied from a few hours to 2 days with GPS data recorded every 15 or 30 s.
12. Point solutions were obtained every 5 min using the Precise Point Positioning (PPP) technique in the GIPSY/OASIS software, estimating site coordinates and tropospheric zenith delay parameters every 5 min and modeling solid-Earth and pole tides [M. King, S. Aoki, *Geophys. Res. Lett.*, **30**, doi:10.1029/2002GL016182 (2003)]. Ocean loading effects were not modeled, but in this region this introduces a maximum error of ~30 mm in the vertical and ~10 mm in the horizontal components. We modeled the site motion as a random walk, constraining the motion to 1 mm $s^{-1/2}$ to maximize the coordinate precisions while not biasing the coordinate estimates. The position precision is 25 mm in each coordinate, based on the weighted root-mean-square of the coordinates of a uniformly moving site.
13. I. M. Whillans, C. R. Bentley, C. J. van der Veen, *Antarct. Res. Ser.* **77**, 257 (2001). Driving stress, the gravitational force acting on the ice, and the transverse distance to resistive shear at the sides of the ice plain were used to derive the speed expected in the absence of basal friction.
14. Differential positions were obtained using the Track software [G. Chen, thesis, Massachusetts Institute of Technology (1998)], estimating site coordinates and a tropospheric zenith delay parameter every 30 s. Fixed reference stations were selected only if their motion in the PPP solutions was linear, and hence any nonlinear motions in the estimated coordinates were assumed to occur at the kinematic site. Site motion was loosely constrained to be less than 0.15 m between consecutive 30-s epochs.
15. Plane wave propagation was assumed. Temporal precision precluded a meaningful four-site source location solution.
16. D. D. Blankenship, C. R. Bentley, S. T. Rooney, R. B. Alley, *J. Geophys. Res.* **92**, 8903 (1986). Trapped-mode propagation of shear or compressional energy (Love or Stoneley waves) in the subglacial layer could explain this low speed of propagation.
17. A (compressional) elastic wave velocity of 3830 m/s was measured upstream of the study area (see 16).
18. One peculiar site was located nearest to the grounded and stagnant Cray Ice Rise. The other two sites were at the upstream limit of the ice plain. One of these was near the rapidly shearing ice stream margin, where some downstream motion always occurred and slip events were subdued in magnitude. The other site, also at this upstream end of the ice plain, sometimes stuck during quiescent periods and sometimes did not.
19. L. Padman, S. Erofeeva, I. Joughin, *Antarct. Sci.* **15**, 31 (2003).
20. We obtained estimates of tidal displacement (and currents) from a numerical tidal model, the Circum-Antarctic Tidal Simulation, version 02.01, CATS02.01, a high-resolution two-dimensional model of barotropic tides of the Southern Ocean and Antarctic Seas [L. Padman, H. A. Fricker, R. Coleman, S. Howard, S. Erofeeva, *Ann. Glaciol.* **34**, 254 (2002)].
21. S. O'Neel, K. A. Echelmeyer, R. J. Motyka, *J. Glaciol.* **47**, 567 (2001).
22. R. A. Walters, W. W. Dunlap, *J. Geophys. Res.* **92**, 8969 (1987).
23. M. F. Meier, A. Post, *J. Geophys. Res.* **99**, 9051 (1987).
24. C. S. M. Doake et al., *Geophys. Res. Lett.* **29**, doi: 10.1029/2001GL014606 (2002).
25. S. Anandakrishnan, D. E. Voigt, R. B. Alley, M. A. King, *Geophys. Res. Lett.* **30**, 1361 (2003).
26. S. Anandakrishnan, R. B. Alley, *J. Geophys. Res.* **102**, 15183 (1997).
27. Although available data (37) do not indicate differences in the till beneath the ice streams consistent with the observed differences in behavior, one cannot rule out that possibility.
28. N. R. Iverson, T. S. Hooyer, R. W. Baker, *J. Glaciol.* **44**, 634 (1998).
29. R. B. Alley, *Geol. Soc. London* **176**, 171 (2000).
30. P. L. Moore, N. R. Iverson, *Geology* **30**, 843 (2002).
31. R. B. Alley, *J. Glaciol.* **39**, 447 (1993).
32. S. Anandakrishnan, R. B. Alley, *Ann. Glaciol.* **20**, 183 (1994).
33. C. R. Bentley, *J. Geophys. Res.* **92**, 8843 (1987).
34. A yield stress of 4 kPa was measured on till extracted from underneath WIS (37).
35. Due to ice stream motion, 0.6 kPa of stress accumulates during a 24.83-hour tidal cycle.
36. Model parameter values are as follows: $H = 750$ m, $L = 100$ km, $V = 500$ m/a, and $E = 10^{10}$ Pa. H and L vary across the ice plain, but the robustness of the model's predictions to the 10% level accommodate most of the real variation in these parameters.
37. B. Kamb, *Antarct. Res. Ser.* **77**, 157 (2001).
38. This work was supported by NSF grant no. 9616394.

27 May 2003; accepted 10 July 2003